# OPTIMAL DESIGN OF PERIODIC ANTIREFLECTIVE STRUCTURES FOR THE HELMHOLTZ EQUATION

By

David C. Dobson

IMA Preprint Series # 965

May 1992

# OPTIMAL DESIGN OF PERIODIC ANTIREFLECTIVE STRUCTURES FOR THE HELMHOLTZ EQUATION

DAVID C. DOBSON*

**Abstract.** We study the problem of designing a periodic interface between two homogeneous materials with different impedance properties, in such a way that time-harmonic waves incident on the interface over a given range of angles have minimal total reflected energy. It is shown that the problem can be "relaxed" to include continuously varying profiles. A simple gradient descent minimization scheme is proposed and examples from several numerical calculations are given.

**Key words.** antireflection, Helmholtz equation, periodic structure.

**AMS(MOS) Subject classifications.** Primary: 49D10, 35R30. Secondary: 65K10, 35J05.

## 1. Introduction.

Often it is desired to design an interface between two regions of different material properties such that an acoustic or electromagnetic wave incident on the interface will have very little energy reflected back. Such an interface is an *antireflective structure.* Examples of antireflective structures in applications are the walls of anechoic chambers used for acoustical measurements, and "moth eye" structures fabricated by microlithographic techniques in optics [12]. Such structures typically exhibit some periodic or "corrugated" pattern.

In this paper, we study the problem of finding periodic antireflective structures, formulated as an optimal design problem for the Helmholtz equation. The goal is to design a periodic interface between two homogeneous regions such that plane waves of a particular frequency, incident over a given range of angles, give rise to minimal *total* reflected energy.

Problems of this type have been studied in the optics and engineering literature (see eg. [9], [12] and the references therein). Most of this previous work has focused on the case of a single incident plane wave; to our knowledge the case of a range of incidence angles (quite important in applications) has not been previously analyzed, except perhaps for the design of multilayer structures. The general approach we have taken is roughly patterned after the recent work of Achdou and Pironneau [1], [2], where a similar problem involving the optimal design of a photocell is studied. Much of the general mathematical framework in [1], [2] is the same for our problem, although their photocell problem involved only a single incident plane wave. The complication caused by allowing a range of incidence angles necessitates many of the new results given here.

The outline of the paper is as follows. In the next section we state the "direct problem": the Helmholtz equation in a periodic structure in $\mathbb{R}^2$. We formulate an equivalent variational problem over a bounded region with "transparent" boundary conditions and show that the problem has a unique solution over a given range of incidence angles, provided that the wavelength of the incident wave is sufficiently large relative to the size of

* Institute for Mathematics and its Applications, University of Minnesota, 514 Vincent Hall, Minneapolis, MN 55455-0436 USA. Research partially supported by a grant from Honeywell, Inc.

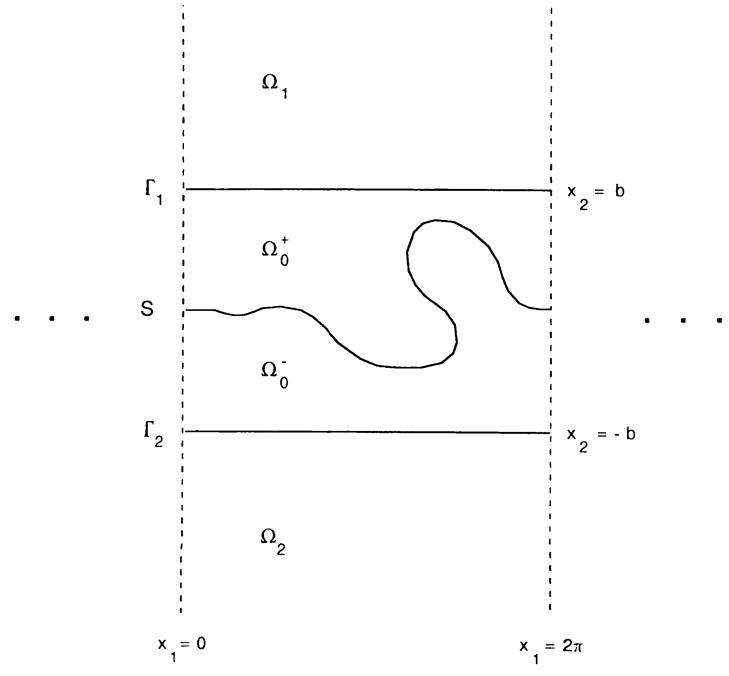


FIG. 1. *Problem geometry.*

the periodic structure. In Section 3, the optimal design problem is stated as a minimization problem. Since the space of curves which define the possible interfaces between the two regions is neither convex nor closed in any natural topology, minimization is extremely difficult. We show that the problem can be "relaxed" to a closed and convex set of continuously varying impedance profiles, over which minimization is much easier. In Section 4, we describe a simple minimization scheme (gradient descent). We then present in Section 5 the results of some numerical experiments in which antireflective interfaces between some different materials are designed.

**2. Periodic Helmholtz equation.** Let $S$ be a simple curve imbedded in the strip

$$\Omega_0 = \{(x_1, x_2) \in \mathbb{R}^2 : -b < x_2 < b\},$$

where $b$ is some positive constant. We assume that $S$ is $2\pi$-periodic with respect to the integers $Z = \{0, \pm 1, \pm 2, \ldots\}$ in the sense that $(S \cap \{x\}) + (2\pi n, 0) = S \cap \{x + (2\pi n, 0)\}$ for all $n \in Z$, $x \in \mathbb{R}^2$. Let $\Omega_1 = \{x \in \mathbb{R}^2 : x_2 > b\}$, $\Omega_2 = \{x \in \mathbb{R}^2 : x_2 < -b\}$. Define the boundaries $\Gamma_1 = \{x_2 = b\}$, $\Gamma_2 = \{x_2 = -b\}$. The curve $S$ divides $\Omega_0$ into two connected components. Denote the component which meets $\Gamma_1$ by $\Omega_0^+$; let $\Omega_0^- = \Omega_0 - \bar{\Omega}_0^+$. The geometry is as pictured in Figure 1.

Suppose that $\mathbb{R}^2$ is filled with material in such a way that the "index of refraction" $k$ satisfies

$$k(x) = \begin{cases} k_1 & \text{in } \Omega_0^+ \cup \bar{\Omega}_1, \\ k_2 & \text{in } \Omega_0^- \cup \bar{\Omega}_2 \end{cases}$$

where $k_1$, $k_2$ are constants, $k_1$ is real and positive, and $Re\ k_2 > 0$, $Im\ k_2 \geq 0$. The case $Im\ k_2 > 0$ accounts for materials which absorb energy (see e.g. [3]). We wish to solve the Helmholtz equation

$$(\triangle + \omega^2 k^2)u = 0 \quad \text{in } \mathbb{R}^2 \tag{1}$$

when an incoming plane wave

$$u_* = e^{i\alpha x_1 - i\beta_1 x_2}$$

is incident on $S$ from $\Omega_1$. Here $\omega$ is the frequency,

$$\alpha = \omega k_1 \sin\theta, \quad \beta_1 = \omega k_1 \cos\theta,$$

and $-\frac{\pi}{2} < \theta < \frac{\pi}{2}$ is the angle of incidence. Notice that $(\triangle + \omega^2 k_1^2)u_* = 0$ in $\bar{\Omega}_1 \cup \Omega_0^+$. Also we note that multiplying the frequency $\omega$ by some $c > 0$ is equivalent to changing the length scale of the problem by a factor of $\frac{1}{c}$.

We are interested in "quasiperiodic" solutions $u$, that is, solutions $u$ such that $ue^{-i\alpha x_1}$ is $2\pi$-periodic. Define $u_\alpha = ue^{-i\alpha x_1}$. It is easily seen that if $u$ satisfies (1) then $u_\alpha$ satisfies

$$(\triangle_\alpha + \omega^2 k^2)u_\alpha = 0 \quad \text{in } \mathbb{R}^2, \tag{2}$$

where the operator $\triangle_\alpha$ is defined by

$$\triangle_\alpha = \triangle + 2i\alpha\partial_1 - |\alpha|^2.$$

We expand $u_\alpha$ in a Fourier series:

$$u_\alpha(x_1, x_2) = \sum_{n \in Z} u_\alpha^n(x_2) e^{inx_1}, \tag{3}$$

where

$$u_\alpha^n(x_2) = \frac{1}{2\pi} \int_0^{2\pi} u_\alpha(x_1, x_2) e^{-inx_1} dx_1.$$

Define for $j = 1, 2$ the coefficients

$$\beta_j^n(\alpha) = e^{i\gamma/2} \left| \omega^2 k_j^2 - (n+\alpha)^2 \right|^{1/2}, \quad n \in Z,$$

where

$$\gamma = \arg(\omega^2 k^2 - (n+\alpha)^2), \quad 0 \leq \gamma < 2\pi.$$

We henceforth assume that $\omega^2 k_j^2 \neq (n+\alpha)^2$ for all $n \in Z$, $j = 1, 2$. It then follows from knowledge of the fundamental solution (see eg. [4], or [6]) that inside $\Omega_1$ and $\Omega_2$, $u_\alpha$ can be expressed as a sum of plane waves:

$$u_\alpha|_{\Omega_j} = \sum_{n \in Z} a_j^n e^{\pm i\beta_j^n(\alpha)x_2 + inx_1}, \quad j = 1, 2, \tag{4}$$

where the $a_j^n$ are complex scalars. Since $\beta_j^n$ is real for at most finitely many $n$, there are only a finite number of *propagating* plane waves in the sum (4); the remaining waves are exponentially damped (or unbounded) as $|x_2| \to \infty$. The exponentially damped waves are called *evanescent*. We will insist that $u_\alpha$ is composed of bounded *outgoing* plane waves in $\Omega_1$ and $\Omega_2$, plus the incident incoming wave $u_*$ in $\Omega_1$. From (3) and (4) we then have the condition that

$$u_\alpha^n(x_2) = \begin{cases} u_\alpha^n(b)e^{i\beta_1^n(\alpha)(x_2-b)}, & n \neq 0, \text{ in } \Omega_1, \\ u_\alpha^0(b)e^{i\beta_1(x_2-b)} + e^{-i\beta_1 x_2} - e^{i\beta_1(x_2-2b)}, & n = 0, \text{ in } \Omega_1, \\ u_\alpha^n(-b)e^{-i\beta_2^n(\alpha)(x_2+b)}, & \text{in } \Omega_2. \end{cases} \tag{5}$$

The unit outward normal $\nu$ on $\Omega_0$ is

$$\nu = \begin{cases} e_2 & \text{on } \Gamma_1, \\ -e_2 & \text{on } \Gamma_2, \end{cases}$$

where $e_2$ is the unit vector in the direction of the $x_2$-axis. From (5) we can then calculate the derivative of $u_\alpha^n(x_2)$ with respect to $\nu$ on $\Omega_0$:

$$\left.\frac{\partial u_\alpha^n}{\partial \nu}\right|_{\Gamma_j} = \begin{cases} i\beta_1^n(\alpha)u_\alpha^n(b), & n \neq 0, \text{ on } \Gamma_1, \\ i\beta_1 u_\alpha^0(b) - 2i\beta_1 e^{-i\beta_1 b}, & n = 0, \text{ on } \Gamma_1, \\ i\beta_2^n(\alpha)u_\alpha^n(-b) & \text{on } \Gamma_2. \end{cases} \tag{6}$$

Thus from (3), (6),

$$\left.\frac{\partial u_\alpha}{\partial \nu}\right|_{\Gamma_1} = \sum_{n\in Z} i\beta_1^n(\alpha)u_\alpha^n(b)e^{inx_1} - 2i\beta_1 e^{-i\beta_1 b}, \tag{7}$$

$$\left.\frac{\partial u_\alpha}{\partial \nu}\right|_{\Gamma_2} = \sum_{n\in Z} i\beta_2^n(\alpha)u_\alpha^n(-b)e^{inx_1}. \tag{8}$$

Since the fields $u_\alpha$ are $2\pi$-periodic in $x_1$, we can move the problem from $\mathbb{R}^2$ to the quotient space (cylinder) $\mathbb{R}^2/(2\pi Z \times \{0\})$. For the remainder of the paper, we shall identify $\Omega_0$ with the cylinder $\Omega_0/(2\pi Z \times \{0\})$, and similarly for the boundaries $\Gamma_j \equiv \Gamma_j/2\pi Z$. Thus from now on, all functions defined on $\Omega_0$ and $\Gamma_j$ are implicitly $2\pi$-periodic in the $x_1$ variable.

For functions $f \in H^{\frac{1}{2}}(\Gamma_j)$ (the Sobolev space of complex valued functions on the circle), define the operator $T_j^\alpha$ by

$$(T_j^\alpha f)(x_1) = \sum_{n\in Z} i\beta_j^n(\alpha)f^n e^{inx_1}, \tag{9}$$

where $f^n = \frac{1}{2\pi}\int_0^{2\pi} f(x_1)e^{-inx_1}$, and equality is taken in the sense of distributions.

LEMMA 2.1. *For $j = 1, 2$, the operator $T_j^\alpha : H^{\frac{1}{2}}(\Gamma_j) \to H^{-\frac{1}{2}}(\Gamma_j)$ is continuous.*

*Proof.* From (9), and the definition of $\beta_j^n(\alpha)$, it is clear that $T_j^\alpha$ is a standard pseudodifferential operator (in fact, a convolution operator) of order one. It follows from general theory (see e.g. [14]) that $T_j$ is continuous. □

From (7), (8) we see that

$$T_j^\alpha(u_\alpha|_{\Gamma_j}) = \frac{\partial u_\alpha}{\partial \nu}|_{\Gamma_j}, \quad j = 1,2,$$

that is, $T_j^\alpha$ is a Dirichlet–Neumann map. We will use the abbreviated notation $T_j^\alpha u_\alpha$ to mean $T_j^\alpha(u_\alpha|_{\Gamma_j})$. We can use the operators $T_j^\alpha$ to define "transparent" boundary conditions on the bounded region $\Omega_0$. It is interesting that the transparent boundary conditions for this problem have such a simple and computationally feasible form, as opposed to the more difficult case for time-domain problems (see eg. [7], [8]).

The scattering problem can be formulated as follows: find $u_\alpha \in H^1(\Omega_0)$ such that

$$(\triangle_\alpha + \omega^2 k^2)u_\alpha = 0 \text{ in } \Omega_0, \tag{10}$$

$$(T_1^\alpha - \frac{\partial}{\partial \nu})u_\alpha = 2i\beta_1 e^{-i\beta_1 b} \text{ on } \Gamma_1, \tag{11}$$

$$(T_2^\alpha - \frac{\partial}{\partial \nu})u_\alpha = 0 \text{ on } \Gamma_2. \tag{12}$$

Notice that conditions (11), (12) already incorporate an "outgoing wave condition". The formulation (10)–(12) admits a variational form. Indeed, taking $v \in H^1(\Omega_0)$, we can restate (10)–(12) in the weak form

$$\begin{aligned} \int_{\Omega_0} \nabla u_\alpha \cdot \nabla \bar{v} &- \int_{\Omega_0} (\omega^2 k^2 - \alpha^2) u_\alpha \bar{v} - 2i\alpha \int_{\Omega_0} (\partial_1 u_\alpha)\bar{v} \\ &- \int_{\Gamma_1} (T_1^\alpha u_\alpha)\bar{v} - \int_{\Gamma_2} (T_2^\alpha u_\alpha)\bar{v} = -\int_{\Gamma_1} 2i\beta_1 e^{-i\beta_1 b}\bar{v} \end{aligned} \tag{13}$$

where $\int_{\Gamma_j}$ represents the dual pairing of $H^{-\frac{1}{2}}(\Gamma_j)$ with $H^{\frac{1}{2}}(\Gamma_j)$.

We now show that (13) admits a unique solution $u_\alpha \in H^1(\Omega_0)$ for a given range on incidence angles, provided that the frequency $\omega$ (or equivalently, the size of the periodic cell) is small enough.

THEOREM 2.2. *Choose some maximum incidence angle $\theta_0$ with $0 \le \theta_0 < \frac{\pi}{2}$. Then there exists a frequency $\omega_0 > 0$ such that the variational problem (13) admits a unique solution $u_\alpha \in H^1(\Omega_0)$ for all incidence angles $\theta$ with $|\theta| \le \theta_0$, and all frequencies $\omega$ with $0 < \omega \le \omega_0$. Furthermore, $\omega_0$ is independent of the shape of the interface $S$.*

*Proof.* Split the operator in (13) into two parts $B_1 + B_2$, where

$$\begin{aligned} B_1(u,v) = \int_{\Omega_0} \nabla u \cdot \nabla \bar{v} + \alpha^2 \int_{\Omega_0} u\bar{v} - 2i\alpha \int_{\Omega_0} (\partial_1 u)\bar{v} \\ - \int_{\Gamma_1} (T_1^\alpha u_\alpha)\bar{v} - \int_{\Gamma_2} (T_2^\alpha u_\alpha)\bar{v} \end{aligned}$$

and

$$B_2(u,v) = -\omega^2 \int_{\Omega_0} k^2 u\bar{v}.$$

Integrating by parts in $x_1$, we see by periodicity that

$$\int_{\Omega_0} (\partial_1 u)\bar{u} = 0.$$

Thus

$$B_1(u,u) = \int_{\Omega_0} |\nabla u|^2 + \alpha^2 \int_{\Omega_0} |u|^2 - \int_{\Gamma_1} (T_1^\alpha u)\bar{u} - \int_{\Gamma_2} (T_2^\alpha u)\bar{u}. \tag{14}$$

For $j = 1,2$, let $\Lambda_j^+(\alpha) = \{n \in Z : Im\ \beta_j^n(\alpha) = 0\}$, $\Lambda_j^-(\alpha) = Z - \Lambda_j^+(\alpha)$. Each $\Lambda_j^+(\alpha)$ is a finite set (corresponding to indices of the propagating outgoing orders), and $0 \in \Lambda_1^+(\alpha)$. We can write

$$-\int_{\Gamma_j} (T_j^\alpha u)\bar{u} = -\int_{\Gamma_j} \sum_{n\in\Lambda_j^+(\alpha)} i\beta_j^n(\alpha) u_n e^{inx_1}\bar{u} - \int_{\Gamma_j} \sum_{n\in\Lambda_j^-(\alpha)} i\beta_j^n(\alpha) u_n e^{inx_1}\bar{u}. \tag{15}$$

Noticing that all $\beta_j^n(\alpha) \in \Lambda_j^-(\alpha)$ satisfy $-i\beta_j^n(\alpha) \geq 0$, we see that the second term on the right-hand side of (15) is real and nonnegative. Furthermore, we have

$$Im\left\{\int_{\Gamma_j} (T_j^\alpha u)\bar{u}\right\} = 2\pi \sum_{n\in\Lambda_j^+(\alpha)} \beta_j^n |u_n|^2.$$

Since $0 \in \Lambda_1^+(\alpha)$, $B_1(u,u)$ satisfies

$$Re\ B_1(u,u) \geq \|\nabla u\|^2_{L^2(\Omega_0)}, \quad -Im\ B_1(u,u) \geq \frac{\beta_1}{2\pi}|u_0|^2,$$

and hence from the definition of $\beta_1$,

$$|B_1(u,u)| \geq \omega c_1 \|u\|^2_{H^1(\Omega_0)}. \tag{16}$$

Thus $B_1$ is a bounded coercive sesquilinear form over $H^1(\Omega_0)$. The Lax-Milgram lemma then gives the existence of a bounded invertible map $A_1 : H^1(\Omega_0) \to H^1(\Omega_0)$ such that $\langle A_1 u, v\rangle_{H^1} = B_1(u,v)$. From (16), $\|A_1^{-1}\| \leq \frac{1}{\omega c_1}$.

Define the operator $A_2 : H^1(\Omega_0) \to H^1(\Omega_0)$ by $\langle A_2 u, v\rangle_{H^1} = \frac{1}{\omega^2} B_2(u,v)$. The operator $A_2$ is bounded and compact. Note that $\|A_2\|$ can be bounded by a constant $c_2$ which depends only on $\|k^2\|_\infty$ (independent of the shape of the interface $S$).

Define $A = A_1 + \omega^2 A_2$. Since $\|A_1^{-1}A_2\| \leq \frac{c_2}{\omega c_1}$, we have

$$\|A^{-1}\| \leq \frac{\|A_1^{-1}\|}{1 - \omega^2\|A_1^{-1}A_2\|} \leq \frac{1}{\omega c_1 - \omega^2 c_2}. \tag{17}$$

Hence, for $\omega > 0$ sufficiently small, $A^{-1}$ exists and is uniformly bounded. □

**3. A minimization problem.** Assume that some maximum incidence angle $\theta_0$ has been chosen. We shall henceforth assume that $\omega$ is such that Theorem 2.2 holds. The assumption that $\omega$ is small is equivalent to assuming that the periodicity of the structure is small compared to the wavelength and is consistent with applications in optics, where "high spatial frequency" structures are of great interest [9], [12]. Notice also that for small $\omega$, we have

$$Im\ \beta_1^n(\alpha) > 0 \text{ for all } n \neq 0. \tag{18}$$

For simplicity, we assume that $\omega$ is such that (18) holds. All of what follows can be extended to the case where $\omega$ is chosen such that $Im\ \beta_1^n(\alpha) > 0$ for all but finitely many $n$, provided that $\omega$ is still small enough that Theorem 2.2 holds.

Under the assumption (18), there is only one propagating outgoing plane wave reflected from the structure for each incident plane wave $u_\alpha^* = e^{i\alpha x_1 - i\beta_1 x_2}$. The coefficient of the reflected wave is

$$r_\alpha = \left( \frac{e^{-i\beta_1 b}}{2\pi} \int_{\Gamma_1} u_\alpha \right) - e^{-2i\beta_1 b}. \tag{19}$$

The energy of the reflected wave is $|r_\alpha|^2$.

The reflected energy $|r_\alpha|^2$ depends implicitly on the surface profile (curve) $S$. For now, we will use the notation $|r_\alpha(S)|^2$. We want to find a curve $S$ which minimizes the total reflected energy over some given range of incidence angles, $\theta \in [\theta_1, \theta_2]$. Thus we wish to minimize the functional

$$J(S) = \int_{\alpha_1}^{\alpha_2} |r_\alpha(S)|^2 d\alpha$$

over some class of "admissible curves" $S$, where $\alpha_1 = \omega k_1 \sin\theta_1, \alpha_2 = \omega k_2 \sin\theta_2$. We do not want to impose artificial constraints on the problem, so we will try to choose a large class of admissible curves.

Let us associate with each surface profile $S$ a function $a_S \in L^\infty(\Omega_0)$ by

$$a_S(x) = \begin{cases} a_1 & \text{if } x \in \Omega_0^+, \\ a_2 & \text{if } x \in \Omega_0^-, \end{cases}$$

where $S$ divides $\Omega_0$ into the disjoint regions $\Omega_0^+$ and $\Omega_0^-$ and $a_j = \omega^2 k_j^2$. We take as admissible curves all $S$ in the class

$$\mathcal{S} = \{S \subset \Omega_0' : S \text{ is a Jordan curve}\},$$

where $\Omega_0' \subset\subset \Omega_0$ is a large subset, chosen to bound the curves $S$ away from the artificial boundaries $\Gamma_1, \Gamma_2$. Define

$$\tilde{\mathcal{A}} = \{a_S \in L^\infty(\Omega_0) : S \in \mathcal{S}\}.$$

The set $\tilde{\mathcal{A}}$ is difficult to minimize over because it is neither convex nor closed in any natural topology. The natural remedy is to minimize instead over the closure of $\tilde{\mathcal{A}}$ with respect to the reflection coefficients $r_\alpha$. Thus, in the terminology of Kohn and Strang [11], we "relax" the problem.

Denote

$$\mathcal{A} = \{a = a_2\gamma + a_1(1-\gamma) : \gamma \in L^\infty(\Omega_0),\ 0 \le \gamma \le 1,\\ \gamma = 0 \text{ above } \Omega_0';\ \gamma = 1 \text{ below } \Omega_0'\}.$$

We have restricted to functions which are constant in the neighborhood $\Omega_0 - \Omega_0'$ of the boundaries $\Gamma_j$ so that the transparent boundary conditions derived in Section 2 are still valid.

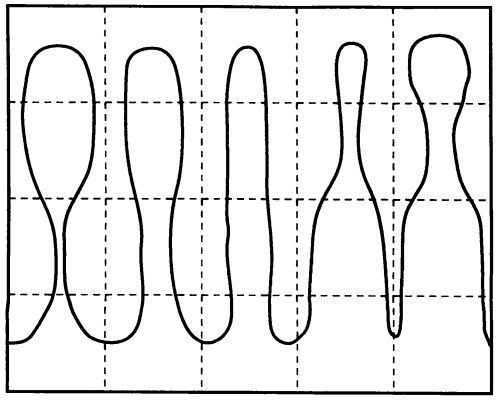

FIG. 2. *Construction of* $a_{S_n} \rightharpoonup a \in \mathcal{A}$.

The set $\mathcal{A}$ is the weak* $L^\infty(\Omega_0)$ closure of $\tilde{\mathcal{A}}$. A sequence $\{a_{S_n}\} \subset \tilde{\mathcal{A}}$ which converges weak* to $a \in \mathcal{A}$ can be constructed as follows. First divide $\Omega_0$ into a uniform grid $\mathcal{G}$ of rectangles. For any given $n$, the grid can be refined enough so that there exists a step function $a_n \in \mathcal{A}$, constant on each rectangle $G \in \mathcal{G}$, such that $|a_n - a| < \frac{1}{n}$ except on a set of measure less than $\frac{1}{n}$. Now take a curve $S_n \in \mathcal{S}$ which passes through each rectangle $G \in \mathcal{G}$, shaped such that $|\int_G (a_{S_n} - a_n)| < \frac{1}{n}$ for all $G \in \mathcal{G}$. An example of how to construct such a curve is shown in Figure 2. It is now straightforward to show that given $g \in L^1(\Omega_0)$ we have $\int_{\Omega_0} g(a_{S_n} - a) \to 0$ as $n \to \infty$.

We note that Theorem 2.2 still applys to problem (10)–(12) when the coefficient $\omega^2 k^2$ is replaced by $a \in \mathcal{A}$. Let the dependence of $r_\alpha$ on the coefficient $a$ be denoted by $r_\alpha[a]$ (that is, $r_\alpha[a]$ is defined by (19) where $u_\alpha$ solves (10)–(12) with $\omega^2 k^2$ replaced by $a$).

THEOREM 3.1. *The set $\mathcal{A}$ is the closure of $\tilde{\mathcal{A}}$ with respect to reflection coefficients. More precisely, for each $a \in \mathcal{A}$, there exists a sequence $a_n \in \tilde{\mathcal{A}}$ such that*

$$r_\alpha[a_n] \to r_\alpha[a].$$

The proof of the theorem is essentially to show that the function $r : \mathcal{A} \to C$ is continuous in the weak* $L^\infty(\Omega_0)$ topology. We require the following lemma. (A similar result is given in Achdou [1]).

LEMMA 3.2. *The quantity $\|u_\alpha\|_{H^1(\Omega_0)}$ is bounded independently of $a \in \mathcal{A}$.*

*Proof.* This follows from the proof of Theorem 2.2, noting that $\|A_2\|$ can be bounded independently of $a \in \mathcal{A}$. □

*Proof.* of Theorem 3.1. Choose a sequence $\{a_n\} \subset \tilde{\mathcal{A}}$ such that $a_n \rightharpoonup a$, weak* $L^\infty(\Omega_0)$. Denote by $u_n$ the solution to problem (13) corresponding to $a_n$. By Lemma 3.2, the sequence $\{u_n\}$ has a weakly convergent subsequence (still denoted $\{u_n\}$): $u_n \rightharpoonup u$ weakly in $H^1(\Omega_0)$ for some $u \in H^1(\Omega_0)$.

Since $u_n \rightharpoonup u$ strongly in $L^2(\Omega_0)$, holding $v \in H^1(\Omega_0)$ fixed, we have $u_n\bar{v} \rightharpoonup u\bar{v}$ strongly in $L^1(\Omega_0)$. Denoting the operator in (13) by $B_a(u,v)$ and using Lemma 2.1, it is then clear that $B_{a_n}(u,v) \rightharpoonup B_{a_n}(u_n,v) = 0$ as $n \rightharpoonup \infty$. Also, since $u\bar{v} \in L^1(\Omega_0)$, we have $B_{a_n}(u,v) \rightharpoonup B_a(u,v)$ as $n \rightharpoonup \infty$. Hence $B_a(u,v) = 0$ for all $v \in H^1(\Omega_0)$. By Theorem 2.2, $u$ is the unique solution to the variational problem (13).

Since $u_n \rightharpoonup u$ weakly in $H^1(\Omega)$, the traces are also convergent: $u_n|_{\Gamma_1} \rightharpoonup u|_{\Gamma_1}$, weakly in $H^{\frac{1}{2}}(\Gamma_1)$. It follows immediately by the definition (19) of $r_\alpha$ that $r_\alpha[a_n] \rightharpoonup r_\alpha[a]$. □

We pose the relaxed minimization problem

$$\min_{a\in\mathcal{A}} J[a] = \int_{\alpha_1}^{\alpha_2} |r_\alpha[a]|^2 d\alpha. \tag{20}$$

THEOREM 3.3. *The minimization problem (20) has at least one solution $a \in \mathcal{A}$.*

*Proof.* This is immediate since $\mathcal{A}$ is weak* $L^\infty$-compact and Theorem 3.1 implies that $r : \mathcal{A} \rightharpoonup C$ is weak* $L^\infty$-continuous. □

**4. A simple minimization method.** In this section, we describe how the method of gradient descent can be applied to find local minima of problem (20). Of course, to perform gradient descent, we must first calculate the gradient. We begin this section with a formal derivation of the gradient.

Let $\delta a$ be a "small" perturbation to the coefficient $a$. We denote the linearization of $J[a]$ with respect to $\delta a$ by $DJ[a](\delta a)$. We have

$$DJ[a](\delta a) = 2Re \int_{\alpha_1}^{\alpha_2} Dr_\alpha[a](\delta a)\bar{r}_\alpha[a]d\alpha, \tag{21}$$

where $Dr_\alpha[a](\delta a)$ denotes the linearization of the reflection coefficient $r_\alpha[a]$ and $\bar{r}_\alpha$ is the complex conjugate. From (19), it is easy to calculate that

$$Dr_\alpha[a](\delta a) = \frac{e^{-i\beta_1 b}}{2\pi} \int_{\Gamma_1} \delta u_\alpha,$$

where $\delta u_\alpha$ solves the linearized problem

$$\begin{aligned} (\triangle_\alpha + a)\delta u_\alpha &= -(\delta a)u_\alpha \quad \text{in } \Omega_0, \\ (T_j^\alpha - \frac{\partial}{\partial \nu})\delta u_\alpha &= 0 \quad \text{on } \Gamma_j, \quad j = 1,2. \end{aligned}$$

The $L^2$ adjoint of the derivative map $Dr_\alpha[a](\cdot)$ is the linear operator $Dr_\alpha^*[a](\cdot)$ which maps complex numbers $\psi$ into $L^2(\Omega_0)$, defined so that

$$Dr_\alpha[a](\delta a) \cdot \bar{\psi} = \int_{\Omega_0} \delta a \cdot \overline{Dr_\alpha^*[a](\psi)} \tag{22}$$

for all $\psi \in \mathcal{C}$. Let $w_\alpha$ solve

$$(\triangle_\alpha + a)w_\alpha = 0 \quad \text{in } \Omega_0, \tag{23}$$

$$(T_1^{\alpha *} - \frac{\partial}{\partial \nu})w_\alpha = -\psi \quad \text{on } \Gamma_1, \tag{24}$$

$$(T_2^{\alpha *} - \frac{\partial}{\partial \nu})w_\alpha = 0 \quad \text{on } \Gamma_2, \tag{25}$$

where $T_j^{\alpha *} f = -\sum i\bar{\beta}_j^n f_n e^{inx}$. An integration by parts argument shows that

$$\int_{\Gamma_1} \delta u_\alpha \cdot \bar{\psi} = \int_{\Omega_0} \delta a \cdot \bar{w}_\alpha u_\alpha.$$

From (22), we then make the identification

$$\overline{Dr_\alpha^*[a](\psi)} = \frac{e^{-i\beta_1 b}}{2\pi} \bar{w}_\alpha u_\alpha. \tag{26}$$

The $L^2$ "gradient" of the functional $J[a]$ is the function $G[a] \in L^2(\Omega_0)$ for which

$$DJ[a](\delta a) = 2Re \int_{\Omega_0} \delta a \cdot \overline{G[a]}. \tag{27}$$

Thus from (21), (22), and (26) we define

$$\overline{G[a]} = \frac{e^{-i\beta_1 b}}{2\pi} \int_{\alpha_1}^{\alpha_2} \bar{w}_\alpha u_\alpha d\alpha,$$

where $w_\alpha$ solves (23)–(25) with $\psi = r_\alpha[a]$.

At any given point $a$, the derivative $DJ[a](\cdot)$ is smallest in the direction of the negative gradient $-G[a]$. The basic gradient descent algorithm is to simply step iteratively in the direction of the negative gradient until (hopefully) the gradient becomes zero (ie. we reach a local minimizer). Since we are constrained to remain in the class of admissible coefficients $\mathcal{A}$, it will be necessary to project inadmissible steps back into $\mathcal{A}$. For this, we define a projection operator $P : L^\infty(\Omega_0) \to \mathcal{A}$ as follows. Given $a \in L^\infty(\Omega_0)$, let

$$\gamma_0 = \frac{Re(a - a_1)Re(a_2 - a_1) + Im(a)Im(a_2)}{|a_1 - a_2|^2}.$$

Define

$$\gamma = \begin{cases} 1 & \text{if } \gamma_0 > 1, \\ 0 & \text{if } \gamma_0 < 0, \\ \gamma_0 & \text{otherwise,} \end{cases}$$

and let $P[a] = a_1(1 - \gamma) + a_2(\gamma)$. The operator $P$ selects the pointwise orthogonal projection onto $\mathcal{A}$.

We now state a simple minimization algorithm:

1. Choose an initial coefficient $a_0$ and an initial step length $t > 0$.
2. Do $k = 0 \ldots$ convergence:
3. If $J[P[a_k - tG[a_k]]] < J[a_k]$ then
   $a_{k+1} = P[a_k - tG[a_k]]$
   Else
   $t = \frac{t}{2}$
   go to step 3.

Since the problem is constrained, it cannot be guaranteed that the gradient $G$ will be zero at a local minimizer. Thus, a reasonable test for convergence in step 2 is that the successive differences in iterates is relatively small, that is $\|a_k - a_{k-1}\|/\|a_0\| < \epsilon$, where $\epsilon > 0$ is some prescribed tolerance.

Conditions under which gradient descent algorithms can be shown to converge (at least for unconstrained problems), along with rates of convergence, etc. are well known and can be found for example in [10]. Generically, when minimizing sufficiently smooth ($C^1$) functionals, one would expect convergence to a local minimizer at a linear rate.

The algorithm stated above is intended as a "first step" toward a robust and practical minimization scheme for this problem. Certainly better minimization algorithms exist (see for example [5]); the virtue of this particular method is simplicity. We expect that quickly convergent schemes which use second order derivative information are likely to require careful regularization, based on a more detailed analysis of the map $a \mapsto r_\alpha$. The design and analysis of minimization methods for this problem and similar problems is an interesting topic for future research. For now, we will not attempt to pursue the issue further, nor will we attempt to analyze the convergence of the method described above.

**5. Numerical experiments.** In this section, we present the results of some numerical experiments carried out with the minimization method presented in Section 4. This is certainly not meant to be a thorough or exhaustive study; we wish only to briefly demonstrate the kinds of results one can expect to obtain using the method of Section 4. Also, we emphasize that the solutions described here are far from complete in an "engineering" sense; the method in its present form is probably less useful as an automatic design tool than as a technique for gaining insight or developing intuition about specific engineering problems.

We now briefly describe the numerical methods used to obtain the results in this section. The "direct problem" (given the coefficient $a$ and incidence $\alpha$, solve (10)-(12) for $u_\alpha$) was solved with a finite element method, derived directly from the variational form (13). The problem was solved over a uniform rectangular grid, with piecewise bilinear basis elements. The coefficients $a$ were parametrized by piecewise constant functions, supported on the cells of the grid. The Dirichlet-Neumann operators $T_j^\alpha$ were approximated by truncation. Because the matrices resulting from the discretized equations were relatively small, the linear system was solved directly by banded Gaussian elimination.

The gradient descent scheme was implemented as described in the previous section, with the solution and gradient replaced by their finite-dimensional counterparts.

In the first two experiments, we try to design periodic interfaces between a glass or plastic substrate, with index of refraction taken to be $k_2 = 1.6$ and air, (with index $k_2 = 1$) which minimize the reflected energy of electromagnetic plane waves of a particular frequency (in the visible or near-infrared optical range) over different ranges of incidence angles. Such a surface would have applications for example in laser optics. As the problem is posed over $\mathbb{R}^2$, we assume that the electromagnetic waves are "TE

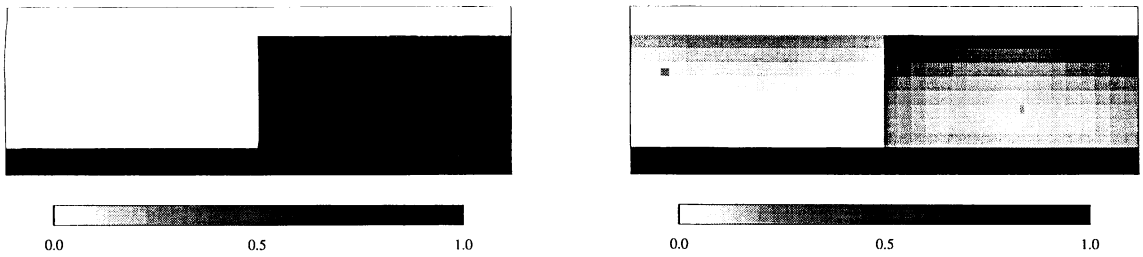


FIG. 3. *a.) Binary initial profile. b.) Profile obtained after 18 iterations.*

polarized", that is, the electric field vector is parallel to the grooves in the grating (see [13] for a discussion of polarization and related topics in optical diffraction gratings, including computational issues).

Figure 3a shows the profile of a so-called "binary" diffraction grating. The dark area represents a substrate volume fraction of one; the light area represents substrate volume fraction equal to zero. We have assumed that the incident wave is in the visible optical range, with wavelength 0.63 $\mu m$ (this is approximately the wavelength of "red" light from a Helium-Neon laser). The scale has been chosen so that the height of the computational box $\Omega_0$ is 0.15 $\mu m$, and the height of the profile is approximately 0.11 $\mu m$. The period of the structure is 0.44 $\mu m$. Optical structures on this scale are often fabricated using microlithographic techniques (see for example [12]). This particular structure is not "tall" enough to have outstanding antireflection properties. Figure 4a shows the reflected energy for the initial profile as a function of incidence angle. The incident wave has been scaled so that it always has unit energy, thus the reflected energy corresponds to the percentage of energy reflected from the structure. This number is called the *reflectivity.* We have chosen the range of incidence angles to be as large as possible, under the constraint that only one outward propagating mode is reflected. The coefficient corresponding to the volume fraction profile in Figure 3a was chosen as the initial guess $a_0$ in the minimization scheme. The method was iterated for 18 steps, resulting in the profile shown in Figure 3b, with reflectivity as shown in 4b. The decrease in total reflectivity across the given range of angles, compared to the initial profile, is by a factor of more than 100, with $|r_\alpha|^2 \leq 2 \times 10^{-4}$ across most of the range. Notice from Figure 3b that the profile begins to resemble a layered structure. Achdou [1] reports a similar layering effect in the photocell design problem.

In the next experiment, we also consider an interface between a substrate with index $k_2 = 1.6$ and air $k_1 = 1$, but we use a lower frequency incident wave, and allow the incidence angles to vary over a much wider range. Here we take incident waves in the near infrared range of 1 $\mu m$, and allow the maximum incidence angle $\theta_0 = 1.2$

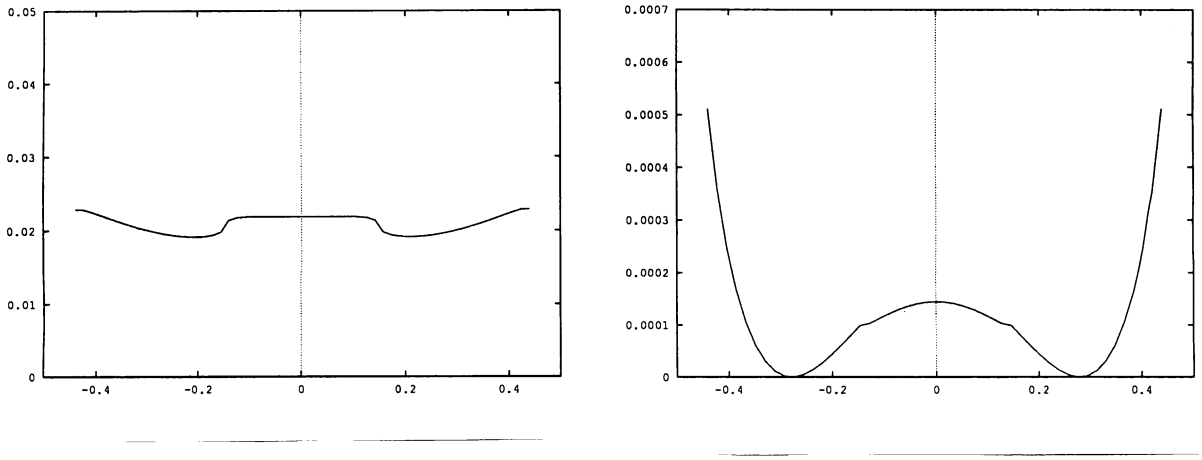


FIG. 4. *a.) Reflectivity vs. incidence angle for the binary initial profile* $a_0$. *b.) Reflectivity for the profile in Fig 3b. Note that the vertical scales are different for the two graphs.*

(radians), or about 69 degrees. As an initial guess $a_0$, we chose the triangular profile illustrated in Figure 5a. The problem is scaled so that the period of the cell is 0.5 $\mu m$. The height of the computational box $\Omega_0$ is 0.41 $\mu m$; the height of the profile is 0.31 $\mu m$. As shown in Figure 6a, the triangular profile is quite antireflective over a small range of angles near 0, with $|r_\alpha|^2 \leq 0.01$, but begins to reflect much more energy as the angle increases toward the "glancing" angle of $\pi/2$. Figure 5b shows the the profile obtained after 45 iterations of the method, with reflectivity shown in Figure 6b. The total reflected energy has been decreased substantially, with reflectivity less than 0.001 (0.1%) across most of the range.

To obtain a more feasible design from a practical point of view—one in which the two materials are not mixed—the profile in Figure 5b could be modified for example by setting

$$\tilde{a} = \begin{cases} a_1 & \text{if } a \leq \frac{1}{2}(a_1 + a_2), \\ a_2 & \text{otherwise.} \end{cases}$$

A graph of the resulting profile is shown in Figure 7. We found that such a modification increased the total reflectivity of the structure (the value of the functional $J[a]$), but actually *decreased* the reflectivity slightly over much of the incidence range. The reflection curve for the modified profile is shown in Figure 8.

For our final experiment, we consider a substrate which absorbs energy, that is, a substrate for which $Im(k_2) > 0$. As in the first example, we have chosen the incident wave with wavelength 0.63 $\mu m$, corresponding to red visible light from a Helium-Neon laser. At this wavelength, silicon (Si) is slightly absorbing, with refractive index $k_2 \approx$

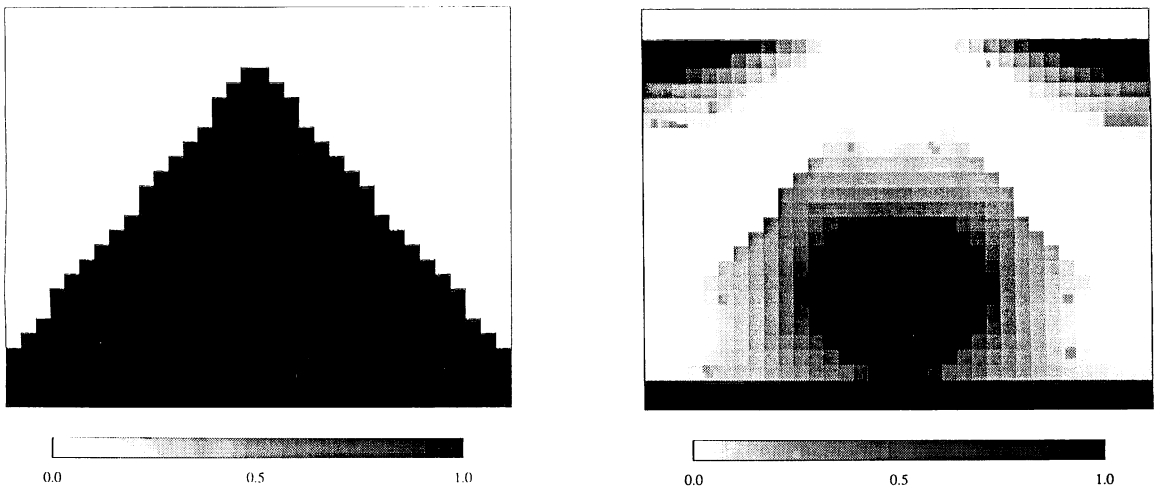


FIG. 5. *a.) Triangular initial profile. b.) Profile obtained after 45 iterations.*

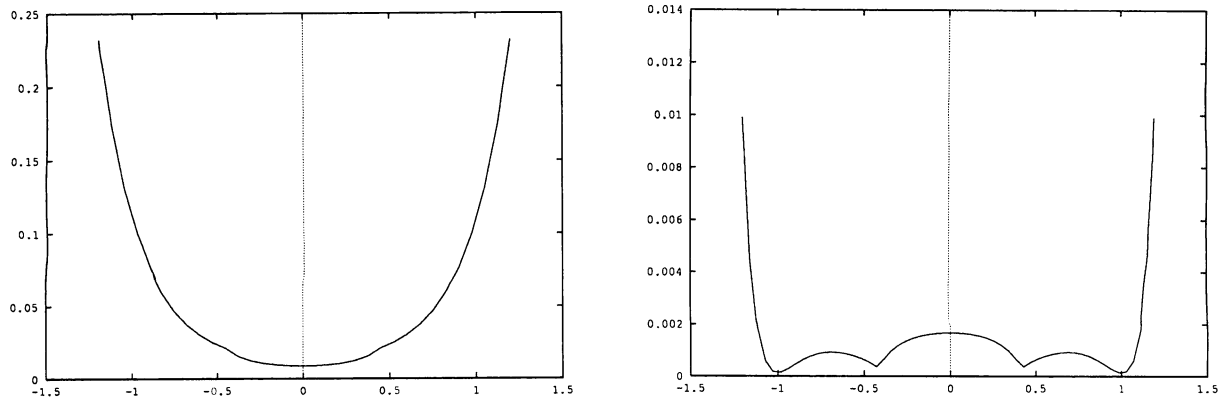


FIG. 6. *a.) Reflectivity for the triangular initial profile. b.) Reflectivity for the profile in Fig 5b.*

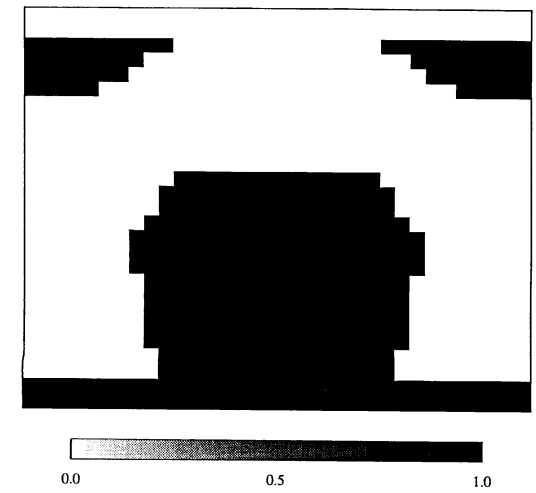


FIG. 7. *Modified version of Figure 5b.*

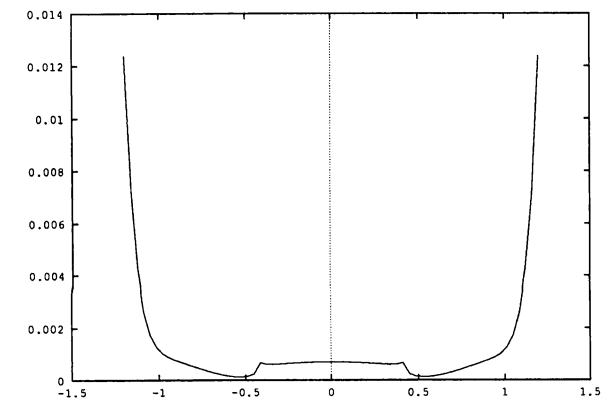


FIG. 8. *Reflectivity for the modified profile in Figure 7.*

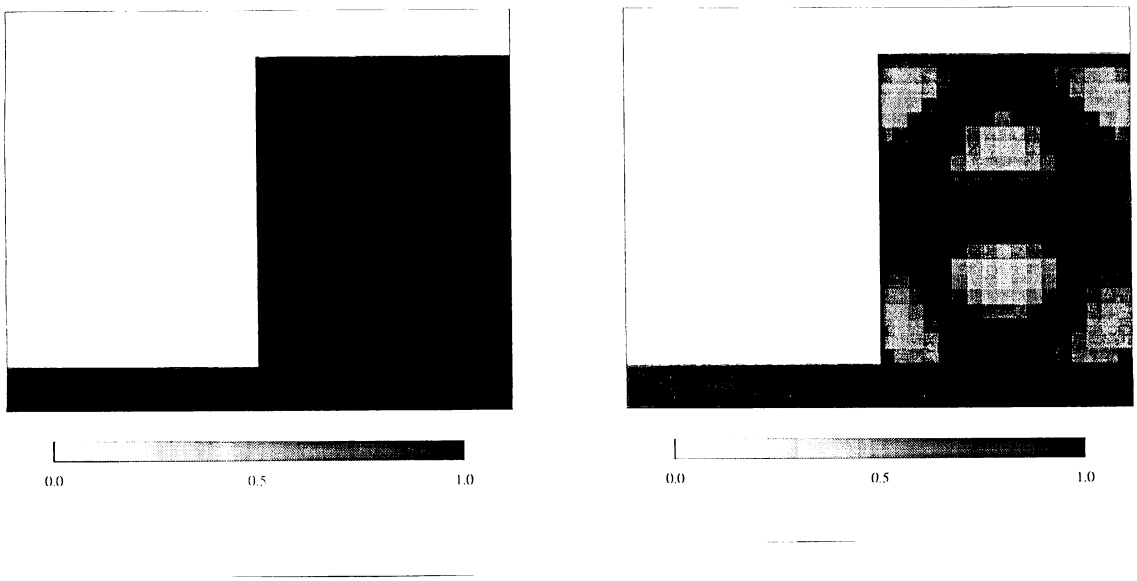


FIG. 9. *a.) Initial silicon profile. b.) Profile obtained after 20 iterations.*

$3.85 + i0.02$. The problem is scaled as in the first example, so that the period of the cell is 0.44 $\mu m$. Figure 9a shows the binary initial profile we took as the initial guess $a_0$. The height of the computational box is 0.37 $\mu m$. The height of the profile is 0.27 $\mu m$. This profile is quite reflective, although less so than a flat profile. The reflected energy versus the incidence angle is shown in Figure 10a. The profile obtained after 20 iterations is shown in Figure 9b. Figure 10b shows the reflected energy versus incidence angle for the final profile. As the figures indicate, although the final profile does not differ greatly from the initial profile, a substantial decrease in reflectivity has been achieved. This seems to indicate that the reflectivity is much more sensitive to changes in the profile when the substrate absorbs energy.

In other experiments, we tried to find antireflective profiles for highly absorbing materials, such as aluminum, nickel, gold, etc., in the visible electromagnetic range. In general, we found these problems to be considerably more difficult, at least in the sense that we failed to find profiles with remarkably low reflectivity properties. This presents an interesting challenge for future research.

Perhaps a more fundamental challenge for the future is to modify, refine, and incorporate these methods into a set of tools which can take into account real engineering design constraints, so that practically realizable antireflective structures can be generated with ease.

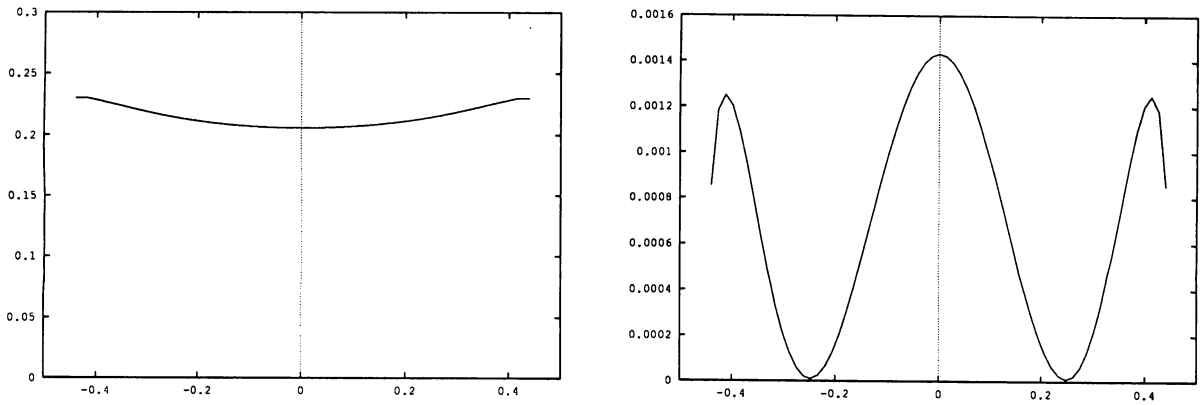


FIG. 10. *a.) Reflectivity for the silicon initial profile. b.) Reflectivity for the profile in Fig 9b.*

## REFERENCES


[1] Achdou, Y., *Numerical optimization of a photocell,* preprint, 1991.

[2] Achdou, Y. and Pironneau, O., *Optimisation d'un capteur d'énergie solaire,* preprint, 1990.

[3] Born, M. and Wolf, E., *Principles of Optics,* sixth edition, Pergamon Press, Oxford, 1980.

[4] Chen, X., and Friedman, A., *Maxwell's equations in a periodic structure,* Trans. Amer. Math. Soc., to appear.

[5] Dennis, J.E., and Schnabel, R. *Numerical Methods for Unconstrained Optimization and Nonlinear Equations,* Prentice Hall, Englewood Cliffs, N.J., 1983.

[6] Dobson, D. and Friedman, A., *The time-harmonic Maxwell equations in a doubly periodic structure,* J. Math. Anal. Appl., to appear.

[7] Engquist, B., and Majda, A., *Radiation boundary conditions for acoustic and elastic wave calculations,* Comm. Pure Appl. Math. **32** (1979), pp. 313-375.

[8] Givoli, D., *Non-reflecting boundary condtions: a review,* J. Comp. Phys., to appear.

[9] Glytsis, E.N., and Gaylord, T.K., *Antireflection surface structure: dielectric layer(s) over a high spatial-frequency surface-relief grating on a lossy substrate,* Appl. Optics, **27** (1988), pp. 4288-4304.

[10] Goldstein, A., *Constructive Real Analysis,* Harper & Row, New York, 1967.

[11] Kohn, R., and Strang, G., *Optimal design and relaxation of variational problems I, II, and III.,* Comm. Pure Appl. Math. **39** (1986), pp. 113-137, 139-182, and 353-377.

[12] Ono, Y., Kimura, Y., Ohta, Y., and Nishida, N., *Antireflection effect in ultrahigh spatial-frequency holographic relief gratings,* Appl. Optics, **26** (1987), pp. 1142-1146.

[13] *Electromagnetic Theory of Gratings,* Topics in Current Physics, Vol. 22, edited by R. Petit, Springer-Verlag, Heidelberg, 1980.

[14] Taylor, M., *Pseudodifferential Operators,* Princeton University Press, Princeton, N.J., 1981.

Recent IMA Preprints

| # | Author/s | Title |
|---|---|---|
| 892 | **E.G. Kalnins, Willard Miller, Jr. and Sanchita Mukherjee** | Models of $q$-algebra representations: the group of plane motions |
| 893 | **T.R. Hoffend Jr. and R.K. Kaul** | Relativistic theory of superpotentials for a nonhomogeneous, spatially isotropic medium |
| 894 | **Reinhold von Schwerin** | Two metal deposition on a microdisk electrode |
| 895 | **Vladimir I. Oliker and Nina N. Uraltseva** | Evolution of nonparametric surfaces with speed depending on curvature, III. Some remarks on mean curvature and anisotropic flows |
| 896 | **Wayne Barrett, Charles R. Johnson, Raphael Loewy and Tamir Shalom** | Rank incrementation via diagonal perturbations |
| 898 | **Mingxiang Chen, Xu-Yan Chen and Jack K. Hale** | Structural stability for time-periodic one-dimensional parabolic equations |
| 899 | **Hong-Ming Yin** | Global solutions of Maxwell's equations in an electromagnetic field with the temperature-dependent electrical conductivity |
| 900 | **Robert Grone, Russell Merris and William Watkins** | Laplacian unimodular equivalence of graphs |
| 901 | **Miroslav Fiedler** | Structure-ranks of matrices |
| 902 | **Miroslav Fiedler** | An estimate for the nonstochastic eigenvalues of doubly stochastic matrices |
| 903 | **Miroslav Fiedler** | Remarks on eigenvalues of Hankel matrices |
| 904 | **Charles R. Johnson, D.D. Olesky, Michael Tsatsomeros and P. van den Driessche** | Spectra with positive elementary symmetric functions |
| 905 | **Pierre-Alain Gremaud** | Thermal contraction as a free boundary problem |
| 906 | **K.L. Cooke, Janos Turi and Gregg Turner** | Stabilization of hybrid systems in the presence of feedback delays |
| 907 | **Robert P. Gilbert and Yongzhi Xu** | A numerical transmutation approach for underwater sound propagation |
| 908 | **LeRoy B. Beasley, Richard A. Brualdi and Bryan L. Shader** | Combinatorial orthogonality |
| 909 | **Richard A. Brualdi and Bryan L. Shader** | Strong hall matrices |
| 910 | **Håkan Wennerström and David M. Anderson** | Difference versus Gaussian curvature energies; monolayer versus bilayer curvature energies applications to vesicle stability |
| 911 | **Shmuel Friedland** | Eigenvalues of almost skew symmetric matrices and tournament matrices |
| 912 | **Avner Friedman, Bei Hu and J.L. Velazquez** | A Free Boundary Problem Modeling Loop Dislocations in Crystals |
| 913 | **Ezio Venturino** | The Influence of Diseases on Lotka-Volterra Systems |
| 914 | **Steve Kirkland and Bryan L. Shader** | On Multipartite Tournament Matrices with Constant Team Size |
| 915 | **Richard A. Brualdi and Jennifer J.Q. Massey** | More on Structure-Ranks of Matrices |
| 916 | **Douglas B. Meade** | Qualitative Analysis of an Epidemic Model with Directed Dispersion |
| 917 | **Kazuo Murota** | Mixed Matrices Irreducibility and Decomposition |
| 918 | **Richard A. Brualdi and Jennifer J.Q. Massey** | Some Applications of Elementary Linear Algebra in Combinations |
| 919 | **Carl D. Meyer** | Sensitivity of Markov Chains |
| 920 | **Hong-Ming Yin** | Weak and Classical Solutions of Some Nonlinear Volterra Integrodifferential Equations |
| 921 | **B. Leinkuhler and A. Ruehli** | Exploiting Symmetry and Regularity in Waveform Relaxation Convergence Estimation |
| 922 | **Xinfu Chen and Charles M. Elliott** | Asymptotics for a Parabolic Double Obstacle Problem |
| 923 | **Yongzhi Xu and Yi Yan** | An Approximate Boundary Integral Method for Acoustic Scattering in Shallow Oceans |
| 924 | **Yongzhi Xu and Yi Yan** | Source Localization Processing in Perturbed Waveguides |
| 925 | **Kenneth L. Cooke and Janos Turi** | Stability, Instability in Delay Equations Modeling Human Respiration |
| 926 | **F. Bethuel, H. Brezis, B.D. Coleman and F. Hélein** | Bifurcation Analysis of Minimizing Harmonic Maps Describing the Equilibrium of Nematic Phases Between Cylinders |
| 927 | **Frank W. Elliott, Jr.** | Signed Random Measures: Stochastic Order and Kolmogorov Consistency Conditions |
| 928 | **D.A. Gregory, S.J. Kirkland and B.L. Shader** | Pick's Inequality and Tournaments |
| 929 | **J.W. Demmel, N.J. Higham and R.S. Schreiber** | Block $LU$ Factorization |
| 930 | **Victor A. Galaktionov and Juan L. Vazquez** | Regional Blow-Up in a Semilinear Heat Equation with Convergence to a Hamilton-Jacobi Equation |
| 931 | **Bryan L. Shader** | Convertible, Nearly Decomposable and Nearly Reducible Matrices |
| 932 | **Dianne P. O'Leary** | Iterative Methods for Finding the Stationary Vector for Markov Chains |
| 933 | **Nicholas J. Higham** | Perturbation theory and backward error for $AX - XB = C$ |
| 934 | **Z. Strakos and A. Greenbaum** | Open questions in the convergence analysis of the lanczos process for the real symmetric eigenvalue problem |
| 935 | **Zhaojun Bai** | Error analysis of the lanczos algorithm for the nonsymmetric eigenvalue problem |
| 936 | **Pierre-Alain Gremaud** | On an elliptic-parabolic problem related to phase transitions in shape memory alloys |
| 937 | **Bojan Mohar and Neil Robertson** | Disjoint essential circuits in toroidal maps |

939 **Bojan Mohar and Svatopluk Poljak** Eigenvalues in combinatorial optimization
940 **Richard A. Brualdi, Keith L. Chavey and Bryan L. Shader**, Conditional sign-solvability
941 **Roger Fosdick and Ying Zhang**, The torsion problem for a nonconvex stored energy function
942 **René Ferland and Gaston Giroux**, An unbounded mean-field intensity model: Propagation of the convergence of the empirical laws and compactness of the fluctuations
943 **Wei-Ming Ni and Izumi Takagi**, Spike-layers in semilinear elliptic singular Perturbation Problems
944 **Henk A. Van der Vorst and Gerard G.L. Sleijpen**, The effect of incomplete decomposition preconditioning on the convergence of conjugate gradients
945 **S.P. Hastings and L.A. Peletier**, On the decay of turbulent bursts
946 **Apostolos Hadjidimos and Robert J. Plemmons**, Analysis of $p$-cyclic iterations for Markov chains
947 **ÅBjörck, H. Park and L. Eldén**, Accurate downdating of least squares solutions
948 **E.G. Kalnins, Willard Miller, Jr. and G.C. Williams**, Recent advances in the use of separation of variables methods in general relativity
949 **G.W. Stewart**, On the perturbation of LU, Cholesky and QR factorizations
950 **G.W. Stewart**, Gaussian elimination, perturbation theory and Markov chains
951 **G.W. Stewart**, On a new way of solving the linear equations that arise in the method of least squares
952 **G.W. Stewart**, On the early history of the singular value decomposition
953 **G.W. STewart**, On the perturbation of Markov chains with nearly transient states
954 **Umberto Mosco**, Composite media and asymptotic dirichlet forms
955 **Walter F. Mascarenhas**, The structure of the eigenvectors of sparse matrices
956 **Walter F. Mascarenhas**, A note on Jacobi being more accurate than QR
957 **Raymond H. Chan, James G. Nagy and Robert J. Plemmons**, FFT-based preconditioners for Toeplitz-Block least squares problems
958 **Zhaojun Bai**, The CSD, GSVD, their applications and computations
959 **D.A. Gregory, S.J. Kirkland and N.J. Pullman**, A bound on the exponent of a primitive matrix using Boolean rank
960 **Richard A. Brualdi, Shmuel Friedland and Alex Pothen**, Sparse bases, elementary vectors and nonzero minors of compound matrices
961 **J.W. Demmel**, Open problems in numerical linear algebra
962 **James W. Demmel and William Gragg**, On computing accurate singular values and eigenvalues of acyclic matrices
963 **James W. Demmel**, The inherent inaccuracy of implicit tridiagonal QR
964 **J.J.L. Velázquez**, Estimates on the $(N-1)$-dimensional Hausdorff measure of the blow-up set for a semilinear heat equation
965 **David C. Dobson**, Optimal design of periodic antireflective structures for the Helmholtz equation
966 **C.J. van Duijn and Joseph D. Fehribach**, Analysis of planar model for the molten carbonate fuel cell
967 **Yongzhi Xu, T. Craig Poling and Trent Brundage**, Source localization in a waveguide with unknown large inclusions
968 **J.J.L. Velázquez**, Higher dimensional blow up for semilinear parabolic equations
969 **E.G. Kalnins and Willard Miller, Jr.**, Separable coordinates, integrability and the Niven equations
970 **John M. Chadam and Hong-Ming Yin**, A diffusion equation with localized chemical reactions
971 **A. Greenbaum and L. Gurvits**, Max-min properties of matrix factor norms
972 **Bei Hu**, A free boundary problem arising in smoulder combustion
973 **C.M. Elliott and A.M. Stuart**, The global dynamics of discrete semilinear parabolic equations
974 **Avner Friedman and Jianhua Zhang**, Swelling of a rubber ball in the presence of good solvent
975 **Avner Friedman and Juan J.L. Velázquez**, A time-dependence free boundary problem modeling the visual image in electrophotography
976 **Richard A. Brualdi, Hyung Chan Jung and William T. Trotter, Jr.**, On the poset of all posets on $n$ elements
977 **Ricardo D. Fierro and James R. Bunch**, Multicollinearity and total least squares
978 **Adam W. Bojanczyk, James G. Nagy and Robert J. Plemmons**, Row householder transformations for rank-$k$ Cholesky inverse modifications
979 **Chaocheng Huang**, An age-dependent population model with nonlinear diffusion in $R^n$
980 **Emad Fatemi and Faroukh Odeh**, Upwind finite difference solution of Boltzmann equation applied to electron transport in semiconductor devices
981 **Esmond G. Ng and Barry W. Peyton**, A tight and explicit representation of $Q$ in sparse $QR$ factorization
982 **Robert J. Plemmons**, A proposal for $FFT$-based fast recursive least-squares
983 **Anne Greenbaum and Zdenek Strakos**, Matrices that generate the same Krylov residual spaces
984 **Alan Edelman and G.W. Stewart**, Scaling for orthogonality
985 **G.W. Stewart**, Note on a generalized sylvester equation
986 **G.W. Stewart**, Updating URV decompositions in parallel